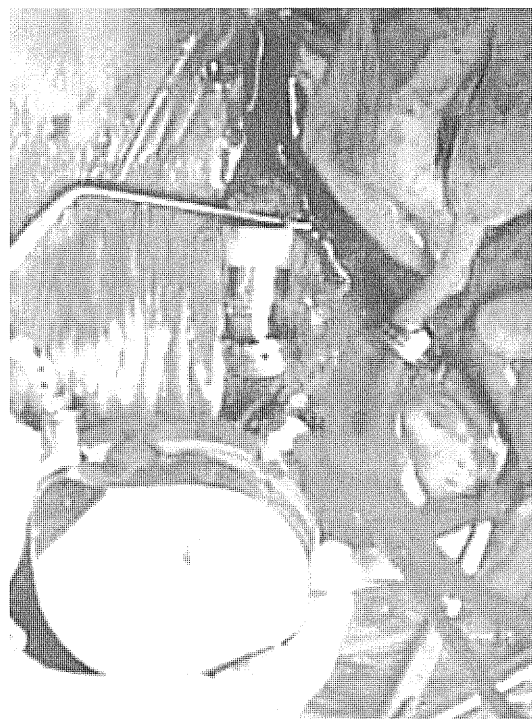


period. Due to the long waiting time for heart donation, conversion to a DuraHeart LVAD was performed. After the DuraHeart implantation, her postoperative recovery was uneventful. The patient was discharged and waited at home for a heart donation.

However, approximately 8 months following the DuraHeart LVAD implantation, the “Mag-Lev Failure” alarm was activated, indicating levitation position errors leading to the failure of the magnetic levitation system. The pump continued to provide the patient with full and stable hemodynamic support by automatically converting to the hydrodynamic bearing rotation mode during this period. The malfunction could not be resolved by exchanging the controllers. We immediately consulted with Terumo Heart, Inc., and exchange of the DuraHeart LVAD was indicated by an analysis of the data downloaded from the controllers.

An emergent operation was arranged. An abdominal midline incision was made along the prior operative incision and extended to the subcostal area. The pump—including the connector nuts of both the outflow and inflow conduits—was freely dissected, and we determined that the exchange could be accomplished without redo sternotomy. Further, a cardiopulmonary bypass (CPB) was established by cannulating the right femoral artery and the right common femoral vein. Immediately after the DuraHeart LVAD was turned off and the outflow conduit was clamped, CPB was initiated. Systemic CPB flow was maintained with a high flow rate and a high perfusion pressure to prevent air embolism. The patient was kept in the Trendelenburg position during the CPB. The operative field was flooded with carbon dioxide. After that, the outflow and the inflow conduits were sequentially disconnected. To control bleeding from the inflow conduit, a suction machine was directly inserted into the conduit and a bloodless field was achieved (Fig. 1). The malfunctioning DuraHeart LVAD, including the driveline, was removed. A new DuraHeart pump was placed, and the outflow conduit was declamped after adequately refilling both the pump and the left ventricle. However, when the systemic flow was transferred from the CPB to the DuraHeart LVAD, adequate flow could not be obtained by the DuraHeart pump. Malposition of the inflow conduit was suspected. While checking the pump flow on the DuraHeart console, the malposition of the inflow conduit was corrected. The inflow conduit was held firmly with a clamp during reconnection to the device in order to prevent another positional change. After that, full systemic flow was obtained and the transfer from the CPB to DuraHeart LVAD was successful. De-airing from the outflow conduit was maintained using a 18G needle after declamping. We continuously monitored the aortic root with transesophageal echocardiography during the procedure, and no air



**Fig. 1** The DuraHeart pump, including the connector nuts of both the outflow and inflow conduits, was freely dissected using a solely subcostal approach without redo sternotomy

entraining was detected. The patient was successfully discharged and had an unremarkable outpatient course.

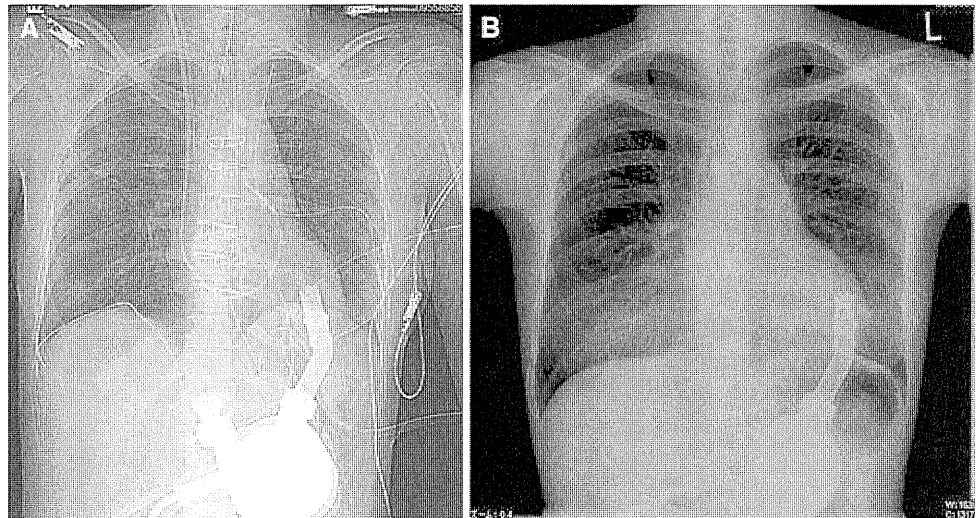
An investigation of the pump and percutaneous cable by Terumo Heart, Inc. identified a fracture on a position sensor wire in the percutaneous cable.

## Discussion

We have presented a case of successful DuraHeart device exchange via a subcostal approach without redo sternotomy. In the operative findings, small segments of the outflow conduit were freely dissected to clamp it and good exposure of both the inflow and outflow connector nuts was needed to disconnect from or reconnect to the device using the wrench. To achieve a bloodless field after the pump was disconnected, a suction machine was inserted directly into the inflow conduit. To prevent air embolism, changes in the patient's position, CPB management, and the de-airing procedure were all carefully performed. Positional correction of the inflow cannula was required to obtain adequate systemic flow when transferring the flow from the CPB to the new DuraHeart LVAD.

Technical considerations associated with LVAD exchange have been previously described [4, 5], and the surgical approach will vary depending on the part, type, and initial technique for implanting the LVAD. A previous

**Fig. 2** A change in the position of the inflow cannula in relation to the left ventricular wall was observed in the present patient by chest radiography. **a** Just after DuraHeart implantation, **b** just before DuraHeart exchange



study indicated that replacing a HeartMate XVE with a HeartMate II can be accomplished with relatively low mortality and morbidity through a subcostal approach, as compared with sternotomy [6]. Based on our present experience, the feasibility of performing DuraHeart LVAD exchange solely by a subcostal approach should be assessed.

The risk of air embolization is a major concern in an LVAD exchange through a subcostal approach. Woo and Acker [7] described a novel continuous intravascular ascending aortic air removal technique that is particularly useful when employing a nonsternotomy approach. A number 6 French pigtail catheter was placed in the ascending aorta through the common femoral artery, exactly above the entry site of the LVAD aortic graft anastomosis. The catheter was connected to the CPB and used as an intra-aortic venting cannula. This simple deairing method would be useful and reliable when using a nonsternotomy approach for LVAD exchange.

Chest radiography revealed reverse ventricular remodeling and a change in the position of the inflow cannula in relation to the left ventricular wall in the present patient (Fig. 2), which were not accompanied by low cardiac output symptoms. We found that correcting the position of the inflow cannula was essential in order to obtain adequate DuraHeart LVAD flow during the operation. The position or direction of the inflow conduit could not be accurately evaluated during the operation, because we could only see the connector nut of the inflow conduit through the operative field (Fig. 1). The pump flow on the DuraHeart console was our sole aid during intraoperative position correction. Therefore, the position of the inflow conduit should be evaluated preoperatively. Raman et al. [8] stated that cardiac computed tomography (CCT) is a useful modality for patients with LVADs, and CCT can detect inflow cannula malpositioning in patients with low cardiac output symptoms. In the current case, CCT could have

provided some supporting information about the inflow cannula before the operation.

In conclusion, we have reported a case of successful DuraHeart LVAD exchange via a subcostal approach. The feasibility of performing this procedure solely through a subcostal approach should be assessed.

## References

1. Miller LW, Pagani FD, Russell SD, John R, Boyle AJ, Aaronson KD, Conte JV, Naka Y, Mancini D, Delgado RM, MacGillivray TE, Farrar DJ, Frazier OH, HeartMate II Clinical Investigators. Use of a continuous-flow device in patients awaiting heart transplantation. *N Engl J Med*. 2007;357(9):885–96.
2. Kirklin JK, Naftel DC, Kormos RL, Stevenson LW, Pagani FD, Miller MA, Ullisney KL, Baldwin JT, Young JB. Third INTERMACS annual report: the evolution of destination therapy in the United States. *J Heart Lung Transpl*. 2011;30(2):115–23.
3. Morshuis M, Schoenbrodt M, Nojiri C, Roefe D, Schulte-Eistrup S, Boergenmann J, Gummert JF, Arusoglu L. DuraHeart magnetically levitated centrifugal left ventricular assist system for advanced heart failure patients. *Expert Rev Med Devices*. 2010;7(2):173–83.
4. Gregoric ID. Exchange techniques for implantable ventricular assist devices. *ASAIO J*. 2008;54(1):14–9.
5. Adamson RM, Dembitsky WP, Baradarian S, Chammas J, Jaski B, Hoagland P, McCalmont V, Ortiz K, Stahovich M, Chillcott S. HeartMate left ventricular assist system exchange: results and technical considerations. *ASAIO J*. 2009;55(6):598–601.
6. Gregoric ID, Bruckner BA, Jacob L, Kar B, Cohn WE, La Francesca S, Frazier OH. Clinical experience with sternotomy versus subcostal approach for exchange of the HeartMate XVE to the HeartMate II ventricular assist device. *Ann Thorac Surg*. 2008;85(5):1646–9.
7. Woo YJ, Acker MA. Implantable ventricular assist device exchange with focused intravascular deairing techniques. *Ann Thorac Surg*. 2011;91(1):306–7.
8. Raman SV, Sahu A, Merchant AZ, Louis LB 4th, Firstenberg MS, Sun B. Noninvasive assessment of left ventricular assist devices with cardiovascular computed tomography and impact on management. *J Heart Lung Transpl*. 2010;29(1):79–85.

# Circulation

JOURNAL OF THE AMERICAN HEART ASSOCIATION

American Heart  
Association®



*Learn and Live*™

**Induced Adipocyte Cell-Sheet Ameliorates Cardiac Dysfunction in a Mouse Myocardial Infarction Model : A Novel Drug Delivery System for Heart Failure**  
Yukiko Imanishi, Shigeru Miyagawa, Norikazu Maeda, Satsuki Fukushima, Satoru Kitagawa-Sakakida, Takashi Daimon, Ayumu Hirata, Tatsuya Shimizu, Teruo Okano, Ichiro Shimomura and Yoshiki Sawa

*Circulation* 2011, 124:S10-S17

doi: 10.1161/CIRCULATIONAHA.110.009993

Circulation is published by the American Heart Association, 7272 Greenville Avenue, Dallas, TX 72514

Copyright © 2011 American Heart Association. All rights reserved. Print ISSN: 0009-7322. Online ISSN: 1524-4539

The online version of this article, along with updated information and services, is located on the World Wide Web at:

[http://circ.ahajournals.org/content/124/11\\_suppl\\_1/S10](http://circ.ahajournals.org/content/124/11_suppl_1/S10)

Data Supplement (unedited) at:

[http://circ.ahajournals.org/content/suppl/2011/09/13/124.11\\_suppl\\_1.S10.DC1.html](http://circ.ahajournals.org/content/suppl/2011/09/13/124.11_suppl_1.S10.DC1.html)

Subscriptions: Information about subscribing to *Circulation* is online at  
<http://circ.ahajournals.org/subscriptions/>

Permissions: Permissions & Rights Desk, Lippincott Williams & Wilkins, a division of Wolters Kluwer Health, 351 West Camden Street, Baltimore, MD 21202-2436. Phone: 410-528-4050. Fax: 410-528-8550. E-mail:  
[journalpermissions@lww.com](mailto:journalpermissions@lww.com)

Reprints: Information about reprints can be found online at  
<http://www.lww.com/reprints>

# Induced Adipocyte Cell-Sheet Ameliorates Cardiac Dysfunction in a Mouse Myocardial Infarction Model

## A Novel Drug Delivery System for Heart Failure

Yukiko Imanishi, PhD; Shigeru Miyagawa, MD, PhD; Norikazu Maeda, MD, PhD; Satsuki Fukushima, MD, PhD; Satoru Kitagawa-Sakakida, MD, PhD; Takashi Daimon, PhD; Ayumu Hirata, MD, PhD; Tatsuya Shimizu, MD, PhD; Teruo Okano, PhD; Iichiro Shimomura, MD, PhD; Yoshiki Sawa, MD, PhD

**Background**—A drug delivery system that constitutively and effectively retains cardioprotective reagents in the targeted myocardium has long been sought to treat acute myocardial infarction. We hypothesized that a scaffold-free induced adipocyte cell-sheet (iACS), transplanted on the surface of the heart, might intramyocardially secrete multiple cardioprotective factors including adiponectin (APN), consequently attenuating functional deterioration after acute myocardial infarction.

**Methods and Results**—Induced ACS were generated from adipose tissue-derived cells of wild-type (WT) mice (C57BL/6J), which secreted abundant APN, hepatocyte growth factor, and vascular endothelial growth factor in vitro. Transplanted iACS secreted APN into the myocardium of APN-knockout (KO) mice at 4 weeks. APN was also detected in the plasma of iACS-transplanted APN-KO mice at 3 months ( $245 \pm 113$  pg/mL). After left anterior descending artery ligation, iACS, generated from either WT (n=40) or APN-KO (n=40) mice, were grafted onto the surface of the anterior left ventricular wall of WT mice, or only left anterior descending artery ligation was performed (n=43). Two days later, inflammation and infarct size were significantly diminished only in the WT-iACS treated mice. One month later, cardiomyocyte diameter and percent fibrosis were smaller, whereas ejection fraction and survival were greater in the WT-iACS treated mice compared with the KO-iACS-treated or nontreated mice.

**Conclusions**—Cardioprotective factors including APN, hepatocyte growth factor, and vascular endothelial growth factor were secreted from iACS. Transplantation of iACS onto the acute myocardial infarction heart attenuated infarct size, inflammation, and left ventricular remodeling, mediated by intramyocardially secreted APN in a constitutive manner. This method might be a novel drug delivery system to treat heart disease. (*Circulation*. 2011;124[suppl 1]:S10–S17.)

**Key Words:** acute myocardial infarction ■ adiponectin ■ cell therapy ■ drug delivery system ■ tissue engineering

Despite recent progress in medical and surgical treatments for heart failure, acute myocardial infarction (AMI) and the subsequent deterioration of cardiac performance is still a major cause of death, worldwide. An array of cardioprotective reagents have been identified to be effective in ameliorating AMI by administrating into the infarcted myocardium in experimental models.<sup>1</sup> However, these reagents have failed to show consistent therapeutic efficacy in several clinical trials, probably due to poor retention or rapid inactivation of reagents in the injured myocardial tissues.<sup>1</sup> Therefore, a drug delivery system (DDS) that retains cardioprotective reagents in the targeted myocardial area has long been sought.

Intramyocardially transplanted autologous stem cells secrete various cardioprotective cytokines and growth factors, enhance

angiogenesis, reduce fibrosis, attenuate apoptosis, and suppress myocyte hypertrophy, consequently ameliorating AMI in a paracrine manner.<sup>2,3</sup> However, cell transplantation for AMI has shown only modest therapeutic efficacy in large-scale clinical studies. It appears to result from insufficient paracrine effects whose magnitude and figure are largely affected by the cell delivery method or transplanted cell source.<sup>4</sup> To enhance the survival and functions of the transplanted cells, we developed a cell-sheet-based delivery method in which isolated cells, cultivated in vitro as a sheet without a scaffold, are simply placed on the surface of the myocardium. This treatment enhances the paracrine effects, resulting in better therapeutic efficacy.<sup>5,6</sup>

Adipocytes differentiated from adipose tissue-derived stromal-vascular fraction (SVF) cells are a promising cell

From the Department of Cardiovascular Surgery (Y.I., S.M., S.F., S.K.-S., Y.S.) and the Department of Metabolic Medicine (N.M., A.H., I.S.), Graduate School of Medicine, Osaka University, Suita, Osaka, Japan; the Division of Biostatistics (T.D.), Department of Mathematics, Hyogo College of Medicine, Nishinomiya, Hyogo, Japan; and the Institute of Advanced Biomedical Engineering and Science (T.S., T.O.), Tokyo Women's Medical University, Shinjuku-ku, Tokyo, Japan.

Presented at the 2010 American Heart Association meeting in Chicago, IL, November 12–16, 2010.

The online-only Data Supplement is available at <http://circ.ahajournals.org/lookup/suppl/doi:10.1161/CIRCULATIONAHA.110.009993/-DC1>.

Correspondence to Yoshiki Sawa, 2-2 Yamada-oka, Suita City, Osaka 565-0871, Japan. E-mail [sawa@surg1.med.osaka-u.ac.jp](mailto:sawa@surg1.med.osaka-u.ac.jp)

© 2011 American Heart Association, Inc.

*Circulation* is available at <http://circ.ahajournals.org>

DOI: 10.1161/CIRCULATIONAHA.110.009993

source for treating AMI because as they secrete hepatocyte growth factor (HGF), vascular endothelial growth factor (VEGF), and, importantly, adiponectin (APN).<sup>7,8</sup> APN is a circulating secretory protein that has multiple cardioprotective effects, including the attenuation of inflammation, fibrosis, and myocyte hypertrophy.<sup>8,9</sup> However, the clinical use of APN for treating AMI has been hampered by the lack of effective systems for delivering APN to the heart. We hypothesized that using cell-sheet technology to deliver adipocytes that secrete multiple cardioprotective factors, including APN, might attenuate the functional deterioration after AMI.

## Methods

Animal care complied with the "Guide for the Care and Use of Laboratory Animals" (NIH publication No. 85 to 23, revised 1996). Experimental protocols were approved by the Ethics Review Committee for Animal Experimentation of Osaka University Graduate School of Medicine.

### Generation and Assessment of Adipocyte Cell-Sheet

The SVF cells of adipose tissue were isolated from wild-type (WT; male C57BL/6J) or APN-knockout (KO) mice,<sup>10</sup> as described previously.<sup>11</sup> The isolated SVF cells were cultured until they become confluent on Ucell dishes (CellSeed Inc, Tokyo, Japan). Differentiation into adipocytes was induced by insulin, dexamethasone, isobutylmethylxanthine, and pioglitazone (Sigma-Aldrich, MO). Incubation at 20°C induced the cells to detach from the culture dishes, yielding a scaffold-free cell-sheet, which we call an "induced adipocyte cell-sheet" (iACS). The secretion of HGF, VEGF, leptin, interleukin (IL)-6, tumor necrosis factor (TNF)- $\alpha$ , and IL-10 into the culture supernatant was assessed by ELISA. Before transplantation, WT mouse-derived iACS (WT-iACS) and APN-KO mouse-derived iACS (KO-iACS) were labeled with the use of a PKH26 kit (Sigma-Aldrich).

### Generation of AMI Model and Cell-Sheet Transplantation

An AMI model was generated by permanent ligation of the left anterior descending artery (LAD) in male C57BL/6J mice, 10 to 15 weeks old.<sup>12</sup> The mice were anesthetized by isoflurane inhalation (Mylan Inc). Five minutes after the LAD ligation, WT-iACS (W group, n=40) or KO-iACS (K group, n=40) was grafted onto the surface of the anterior left ventricular (LV) wall, or a sham operation was performed (C group, n=43). The mice were euthanized at 2 and 28 days after LAD ligation and cell-sheet transplantation.

### Assessment of Cardiac Function and Survival

Cardiac function was assessed with the use of an echocardiography system equipped with a 12-MHz transducer (GE Healthcare) at 4 weeks. The LV dimensions were measured, and LV ejection fraction was calculated as  $(LVd^3 - LVS^3) / LVd^3 \times 100$ , where LVd and LVS are the LV end-diastolic and end-systolic dimensions, respectively.<sup>12</sup> The mice were housed in a temperature-controlled incubator for 50 days after treatment to determine their survival.

### Histological Analysis

Freshly excised hearts were stained with 1% 2,3,5-triphenyltetrazolium chloride (TTC; Sigma-Aldrich). The red-stained infarct area was quantified by computerized planimetry, using MetaMorph Software (Molecular Devices). Frozen sections (8  $\mu$ m) of hearts and cell-sheets were stained with antibodies against APN (Otsuka Pharmaceutical, Tokushima, Japan) or CD11b (Abcam, Cambridge, UK). The secondary antibody was Alexa 488 goat anti-rabbit (Life Technologies). Counterstaining was performed with 6-diamidino-2-phenylindole (Life Technologies). To analyze the myocardial colla-

gen accumulation, heart sections were stained with Masson trichrome. The collagen volume fraction was calculated in the peri-infarct area. To assess cardiomyocyte diameter, heart sections were stained with periodic acid-Schiff. MetaMorph Software was used for the quantitative morphometric analysis.

### Cytokine Antibody Array

Proteins were isolated from whole-heart samples and analyzed using a Milliplex Mouse Cytokine/Chemokine Panel Premixed 32Plex, according to the manufacturer's instructions (Millipore).

### Quantitative Real-Time PCR

Total RNA was isolated from the peri-infarct area by use of the RNeasy Mini Kit and reverse-transcribed, using Omniscript Reverse transcriptase (Qiagen, Hilden, Germany). Quantitative PCR was performed with the PCR System (Life Technologies). The expression of each mRNA was normalized to that of glyceraldehyde-3-phosphate dehydrogenase.

### Statistical Analysis

Data are expressed as the mean  $\pm$  SEM. The data distributions were checked for normality with the Shapiro-Wilk test and for equality of variances with the Bartlett test. Comparisons between 2 groups were made using the unpaired *t* test or the Wilcoxon-Mann-Whitney *U* test, as appropriate. For comparisons among 3 groups, we used 1-way ANOVA, followed by Fisher protected least-significance difference test or the Kruskal-Wallis test, followed by the post hoc pairwise Wilcoxon-Mann-Whitney *U* test, as appropriate. The survival curves were prepared by using the Kaplan-Meier method and were compared using the overall log-rank test, followed by the post hoc pairwise log-rank test. The multiplicity in pairwise comparisons was corrected by the Benjamin-Hochberg procedure. All probability values are 2-sided, and values of  $P < 0.05$  were considered to indicate statistical significance. Statistical analysis was performed with the StatView 5.0 Program (Abacus Concepts, Berkeley, CA) and the R program.<sup>13</sup>

An expanded Methods section can be found in the online-only Data Supplement.

## Results

### Characterization of the Adipocyte Cell-Sheets

Most SVF cells differentiated into mature adipocytes bearing oil droplets by 7 days after differentiation induction. Induced ACS or undifferentiated SVF cell-sheets were then generated by lowering the temperature (Figure 1A). Each iACS was approximately 7 mm in diameter (Figure 1B) and 100  $\mu$ m thick (Figure 1C). WT-iACS expressed abundant APN in the cytoplasm and extracellular matrix around the oil-droplet-rich adipocytes, as assessed by immunohistochemistry (Figure 1D) and ELISA (Figure 1E). In contrast, neither the SVF cell-sheets of either origin nor the KO-iACS expressed APN (Figure 1D and 1E). The ELISA showed abundant HGF expression in WT-iACS and KO-iACS, which was down-regulated compared with the WT SVF cells (Figure 1F). The secretion of VEGF and leptin was remarkably enhanced by the SVF cell differentiation into adipocytes. IL-6 and IL-10 were secreted by the WT-iACS and WT-SVF cells at similar levels, which were lower than the levels secreted by KO-iACS. The secretion of TNF- $\alpha$  was not evident in any group because the cell-free culture medium also contained 2.29 pg/mL TNF- $\alpha$ .

### Transplanted Induced ACS Supplied APN to the Myocardium

WT-iACS were transplanted onto the heart of intact APN-KO mice to evaluate behavior of the WT-iACS, including APN

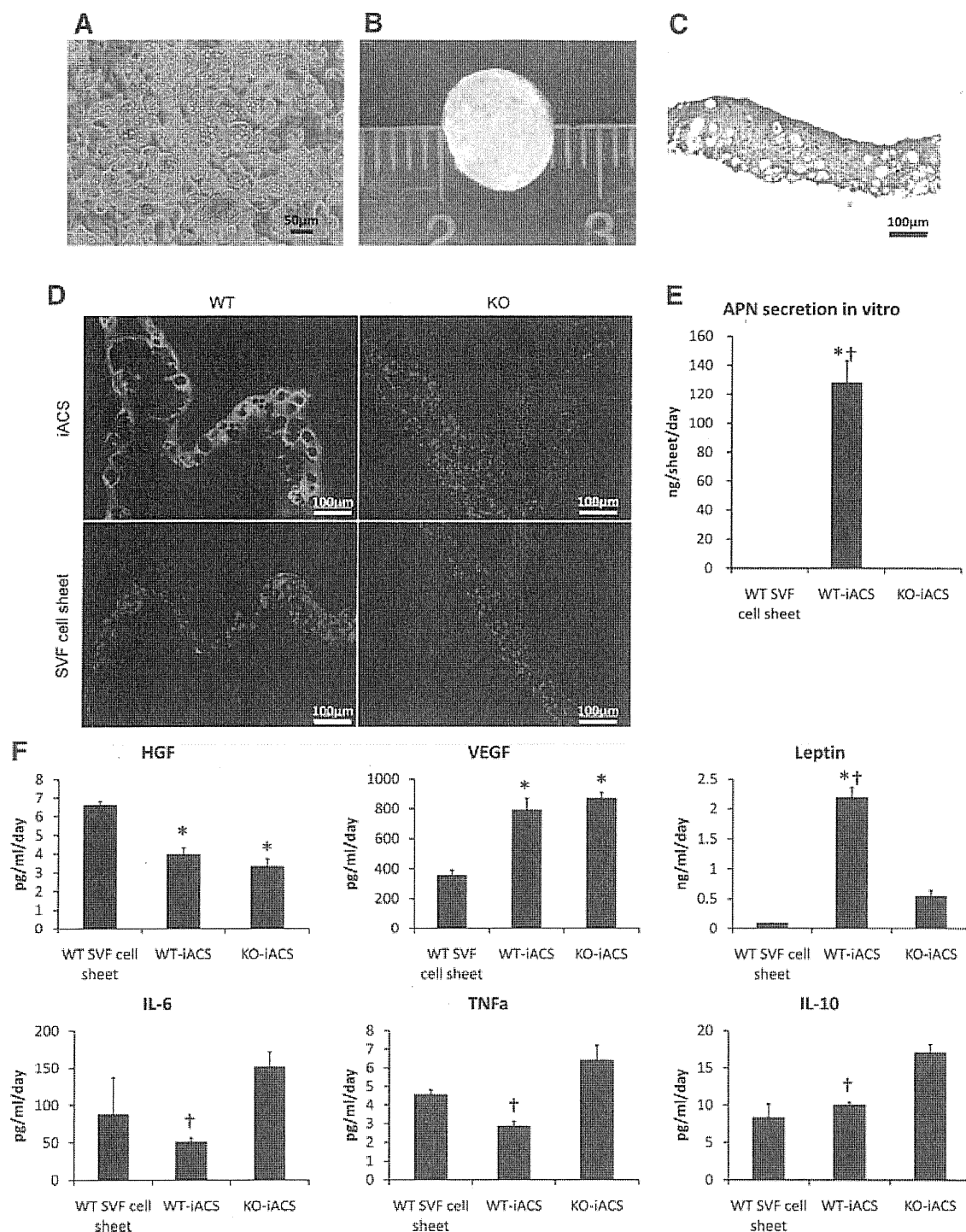


**Figure 1.** Characterization of induced adipocyte cell-sheet (iACS) in vitro. **A**, Histological analysis showing mature adipocytes with oil droplets in the cytosol. **B**, Induced ACS detached from the temperature-responsive culture dish. **C**, Cross-sectional view of hematoxylin and eosin-stained iACS. **D**, Representative pictures of adiponectin (APN)-stained cell-sheets. Wild-type (WT)-iACS showed strong labeling for APN. The WT stromal-vascular fraction (SVF) cell-sheet, knockout (KO)-iACS, and KO SVF cell-sheet were negative for APN. Green indicates APN; blue, nuclei. **E**, APN secretion into the WT-iACS culture supernatant determined by ELISA (WT SVF cell sheet,  $n=2$ ; WT-iACS,  $n=5$ ; KO-iACS,  $n=8$ ;  $P<0.05$ , Kruskal-Wallis test). \* $P<0.05$  versus WT SVF cell-sheet, † $P<0.05$  versus KO-iACS, post hoc Wilcoxon-Mann-Whitney  $U$  test. **F**, Hepatocyte growth factor (HGF), vascular endothelial growth factor (VEGF), leptin, interleukin (IL)-6, IL-10, and tumor necrosis factor (TNF)- $\alpha$  secretion into the culture supernatant, measured by ELISA. WT-iACS secreted HGF, VEGF, leptin, IL-6, and IL-10 but not TNF- $\alpha$  (WT SVF cell sheet,  $n=2$ ; WT-iACS,  $n=8$  to 12; KO-iACS,  $n=6$  to 9). HGF, VEGF, and leptin ( $P<0.05$ , ANOVA); \* $P<0.05$  versus WT SVF cell-sheet, † $P<0.05$  versus KO-iACS, post hoc Fisher protected least-significance difference test. TNF- $\alpha$ , IL-6, and IL-10 ( $P<0.05$ , Kruskal-Wallis test); \* $P<0.05$  versus WT SVF cell-sheet, † $P<0.05$  versus KO-iACS, post hoc Wilcoxon-Mann-Whitney  $U$  test.

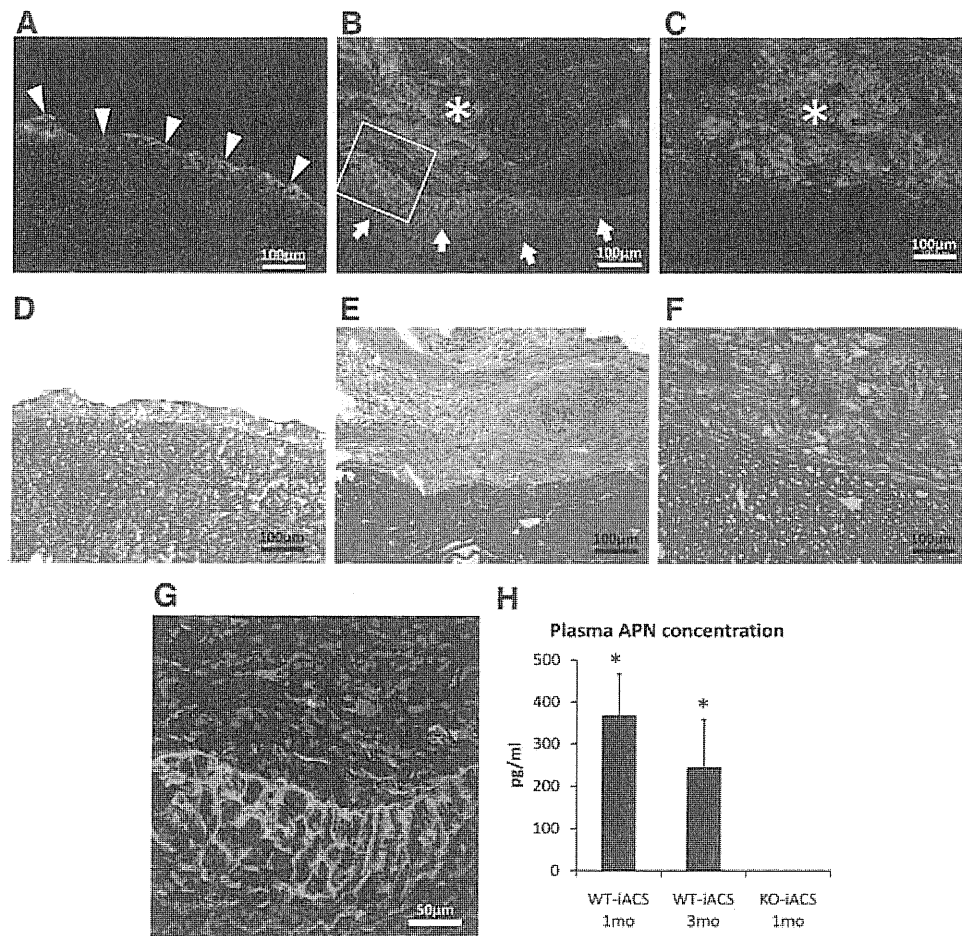


**Figure 2.** Local and systemic delivery of induced adipocyte cell-sheet (iACS)-derived adiponectin (APN) in vivo. **A**, Immediately after wild-type (WT)-iACS implantation onto the knockout (KO) mouse heart, iACS-expressed APN was detected on the epicardium. Arrowheads show the implanted WT-iACS. Green indicates APN; blue, nuclei. **B**, WT-iACS stained with red fluorescent dye were implanted onto KO myocardium. Twenty-eight days after transplantation, APN was detected both in the surviving WT-iACS and the extracellular matrix (ECM) of the KO mouse myocardium at the implanted site. Asterisk indicates the implanted WT-iACS. Arrows show iACS-derived APN in the host myocardium. **C**, KO-iACS stained with red fluorescent dye and implanted onto KO myocardium. Twenty-eight days after transplantation, the implanted KO-iACS survived, but no APN was detected in the KO-iACS or the ECM. Asterisk indicates the implanted KO-iACS. Green indicates APN; red, KO-iACS; and blue, nuclei. **D** through **F**, Hematoxylin and eosin staining of a serial section from the sample in **A**, **B**, and **C**, respectively. **G**, High-magnification image of the square in **B** and **H**. Plasma APN concentration of WT-iACS (WT) or KO-iACS (KO) recipient APN-KO mice. APN was detected in the WT group plasma 1 (n=4) and 3 months (n=3) after transplantation but not in the KO group plasma (n=4,  $P < 0.05$ , Kruskal-Wallis test). \* $P < 0.05$  versus KO 1 month, post hoc Wilcoxon-Mann-Whitney *U* test.

production. Immediately after transplantation, the WT-iACS expressed APN epicardially at the anterior LV wall, but it was not expressed intramyocardially (Figure 2A). Four weeks after transplantation, the WT-iACS had survived, was approximately 600  $\mu\text{m}$  thick, and contained adipocytes and connective tissue. At this time, the WT-iACS was tightly integrated with the epicardium, but no invasion of transplanted cells into the recipient myocardium was observed (Figure 2B and 2E). APN was expressed in the cytoplasm of scattered surviving WT-iACS cells and in the myocardium close to the WT-iACS (Figure 2B and 2G). In contrast, although the KO-iACS transplanted into KO mice survived (Figure 2C and 2F), they did not express or secrete APN (Figure 2C). When WT-iACS was transplanted into KO mice, APN was detected in the plasma 1 and 3 months later, but it was not detected in the plasma of KO mice with the KO-iACS implant (Figure 2H).

### Induced ACS Implantation Reduced Inflammatory Responses and Infarct Area 2 Days After MI

The anti-inflammatory effects of WT-iACS were evaluated by cytokine antibody array analysis of whole-heart lysates from the AMI mice that were treated with WT-iACS (W), KO-iACS (K), or no iACS (C) groups at 2 days after implantation (Table). A significantly lower level of the inflammatory factor granulocyte macrophage colony-stimulating factor (GM-CSF) was observed in the W group compared with the others, and the levels of other inflammatory cytokines, keratinocyte chemoattractant, IL-6, granulocyte (G)-CSF, and monocyte chemoattractant protein-1 (MCP-1) showed a trend toward downregulation in the W group. Quantitative RT-PCR showed that the TNF $\alpha$  mRNA levels were lower in the peri-infarct area of the W group than in that of the K and C groups, which reached statistical significance in the W group (Figure 3A). Furthermore, immunohistochem-

**Table. Cytokine Antibody Array**

	W Group (n=4)	K Group (n=5)	C Group (n=6)
Granulocyte macrophage colony-stimulating factor, pg	0.0±0*†	21.8±1.3	18.5±6.7
Keratinocyte chemoattractant, pg	292.7±42.7	539.9±56.4	629.9±113.1
Interleukin-6, pg	175.3±16.0	295.3±44.0	281.4±51.5
Granulocyte-colony stimulating factor, pg	37.6±5.7	94.6±35.0	52.8±9.5
Monocyte chemoattractant protein-1, pg	316.4±51.9	467.6±50.4	388.7±87.1

$P < 0.05$ , Kruskal-Wallis test.

\* $P < 0.05$  versus C group.

† $P < 0.05$  versus K group, post hoc Wilcoxon-Mann-Whitney *U* test.

istry for CD11b showed significantly fewer infiltrated macrophages in the peri-infarct area of the W and K groups than in that of the C group (Figure 3B). Finally, a semiquantitative assessment by TTC staining showed that the infarct area was significantly smaller in the W group than in the K and C groups (Figure 4).

### Induced ACS Transplantation Suppressed LV Remodeling Development at 4 Weeks After MI

Four weeks after LAD ligation, the C group showed a typical MI with a large anterior LV scar, dilatation of the LV cavity, and cardiomyocyte hypertrophy. By comparison, the LV of the W group was less dilated, and the anterior wall was thicker (Figure 5A). The diameter of the cardiomyocytes was significantly smaller in the W group (Figure 5B and 5C), and there was less collagen accumulation (Figure 5D and 5E). There was no difference in capillary density among the groups (online-only Data Supplement Figure 1).

### Therapeutic Effects of Induced ACS Transplantation on Cardiac Performance and Survival at 4 Weeks After MI

Cardiac performance was evaluated by 2D echocardiography 4 weeks after implantation. Both the diastolic and systolic LV

dimensions were smaller in the W group than the others, but the difference was not significant. In contrast, LV ejection fraction was significantly greater in the W group than the K and C groups (Figure 6A). In addition, in a WT-iACS-transplanted rat model of acute MI, invasive hemodynamic analysis showed higher end-systolic pulmonary vascular resistance and  $dp/dt_{max}$  and lower  $dp/dt_{min}$ , compared with sham transplantation (online-only Data Supplement Figure 2). Mortality was substantial until 14 days after LAD ligation in the K and C groups. In contrast, in the W group, there was little mortality 5 days after MI and thus a significant difference in survival (Figure 6B).

### Discussion

We developed an adipocyte cell-sheet-based DDS for the heart. These sheets, which are generated from adipose tissue-derived SVF cells induced to differentiate in culture, secreted multiple cardioprotective factors in vitro, including APN, HGF, and VEGF. Although adipose tissue-derived SVF cells had no ability to secrete APN, after the differentiation to adipocytes, the cells started to secrete APN in addition to HGF and VEGF. APN was secreted from the iACS into the myocardium and blood for at least 3 months, probably along with HGF, VEGF, leptin, and IL-10. In a mouse model of AMI, WT-iACS significantly decreased inflammation and myocardial infarct size at the acute stage. Furthermore, myocardial fibrosis and cardiomyocyte hypertrophy were significantly attenuated at the late stage, which led to improved cardiac performance and a better post-MI survival rate. Importantly, the transplantation of KO-iACS onto infarcted hearts resulted in only modest therapeutic benefits, indicating that APN plays a pivotal role in attenuating the AMI in this experimental model.

There have been many experimental and clinical studies in which the administration of exogenous proteins, including APN, induced angiogenesis, reversed remodeling, and improved cardiac function.<sup>1,14</sup> The issues in this method may be that naked protein is delivered to the heart and is often poorly retained or quickly inactivated and therefore lacks long-term efficacy.<sup>15</sup> MI is a progressive disease, characterized by massive ischemic necrosis of the myocardial tissue and subsequent inflammation. This leads to cardiac remodeling that exacerbates the oxygen shortage in the surviving cardiac tissue. These pathological and functional deteriorations eventually cause end-stage heart failure. A constitutive and balanced supply of cardioprotective reagents, rather than the 1-time administration of a single reagent, should inhibit this vicious circle. The direct injection of plasmid vectors encoding targeted reagents and the transplantation of genetically modified cells can provide a controlled and stable supply of reagents over the long term; however, their clinical use is limited because the safety of the viral systems used as vectors for the plasmids and of modifying cells for transplant is still a concern.<sup>16</sup> Encapsulation as the DDS for biomaterials is another attractive approach; however, difficulty in controlling the rate of reagent release, such as the occurrence of an initial burst release, limits its therapeutic efficacy.<sup>17,18</sup> In addition, biodegradable polymers that carry reagents may induce the deposition of extracellular matrix and myocardial inflamma-

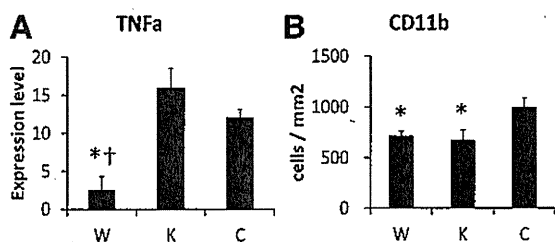


**Figure 3.** Induced adipocyte cell-sheet (iACS) effects on inflammatory responses after myocardial infarction at the implant/myocardium border zone 2 days after implantation. **A**, Quantitative RT-PCR results for the tumor necrosis factor (TNF)- $\alpha$  transcript. TNF- $\alpha$  transcription was significantly lower in the W group (n=4) than in the K (n=4) and C groups (n=6,  $P < 0.05$ , Kruskal-Wallis test) \* $P < 0.05$  versus C group, † $P < 0.05$  versus K group, post hoc Wilcoxon-Mann-Whitney *U* test. **B**, Quantification of CD11b-positive cells. The number of CD11b-positive cells was significantly lower in the W (n=4) and K (n=4) groups than in the C group (n=6,  $P < 0.05$ , ANOVA). \* $P < 0.05$  versus C group, Fisher protected least-significance difference test.



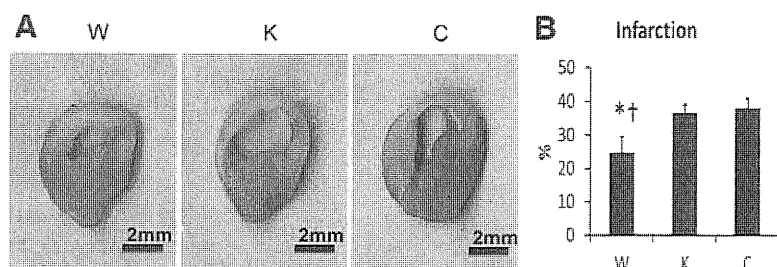


**Figure 4.** Infarct area of induced adipocyte cell-sheet (iACS)-treated heart 2 days after myocardial infarction. **A**, Representative 2,3,5-triphenyltetrazolium chloride staining images at border zone of infarct. **B**, Quantification of infarct size. The percent infarcted area was significantly lower in the W group ( $n=8$ ) compared with the other groups (K,  $n=7$ ; C,  $n=9$ ;  $P<0.05$ , ANOVA). \* $P<0.05$  versus C group. † $P<0.05$  versus K group, Fisher protected least-significance difference test.

tion, leading to pathological fibrotic states.<sup>19</sup> Our cell-sheet-based DDS constitutively and effectively delivered multiple cardioprotective factors over the long term, leading to reverse LV remodeling after MI, without gene modification or scaffold use. Thus, this strategy might be more practical and effective than other methods for delivering therapeutic proteins for treating MI in the clinical arena.

It is possible that the delivery of multiple growth factors will improve therapeutic efficacy over the delivery of a single factor. This hypothesis is supported by a study showing that the combination of HGF and VEGF leads to better engraftment and significant angiogenesis, compared with either factor alone.<sup>20</sup> In our study, the KO-iACS, which secreted HGF and VEGF but not APN, reduced macrophage infiltration but did not induce functional or survival benefits. These benefits were conferred by the WT-iACS, which produced APN, suggesting that APN's benefits are different from and

in addition to those of known paracrine mediators, such as HGF or VEGF.

APN is a protective factor against cardiovascular diseases.<sup>9,21</sup> In particular, its anti-inflammatory properties may be the major reason for its beneficial effects on cardiovascular disorders, because APN-deficient mice exhibit increased TNF- $\alpha$  production and myocardial apoptosis in response to ischemia reperfusion.<sup>22,23</sup> We observed that the expression of TNF- $\alpha$  in the AMI heart was significantly reduced by transplanting WT-iACS but not KO-iACS, which secrete similar levels of the same cytokines, except for APN, suggesting that the direct anti-inflammatory effects of APN played a key role in the attenuated inflammation in this study. In addition, the infarct size was significantly smaller in the WT-iACS-transplanted hearts than in the KO-iACS-transplanted ones. Infarct size is determined by multiple factors, including the magnitude of ischemic stimuli, degree of

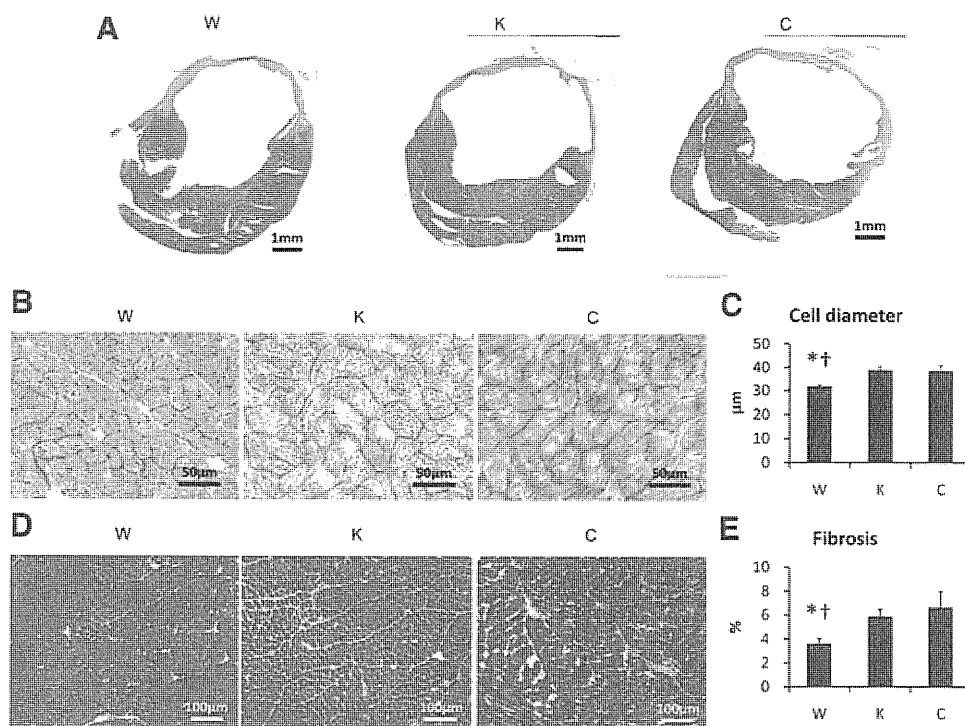


**Figure 5.** Effects on left ventricular remodeling by induced adipocyte cell-sheet (iACS) transplantation 4 weeks after myocardial infarction. **A**, Representative macro images from each group. **B**, Representative periodic acid-Schiff staining of tissue remote from infarct site. **C**, Quantification of cardiomyocyte diameter. Cardiomyocyte diameters in the tissue remote from the infarct site were significantly smaller in the W group ( $n=6$ ) than in the other groups (K,  $n=8$ ; C,  $n=5$ ;  $P<0.05$ , ANOVA). \* $P<0.05$  versus C group. † $P<0.05$  versus K group, Fisher protected least-significance difference test. **D**, Representative Masson trichrome staining images at the border area. **E**, Quantification of percent fibrosis. Fibrosis at the border area was significantly suppressed in the W group ( $n=6$ ) compared with the other groups (K,  $n=8$ ; C,  $n=5$ ;  $P<0.05$ , Kruskal-Wallis test). \* $P<0.05$  versus C group. † $P<0.05$  versus K group, post hoc Wilcoxon-Mann-Whitney  $U$  test.

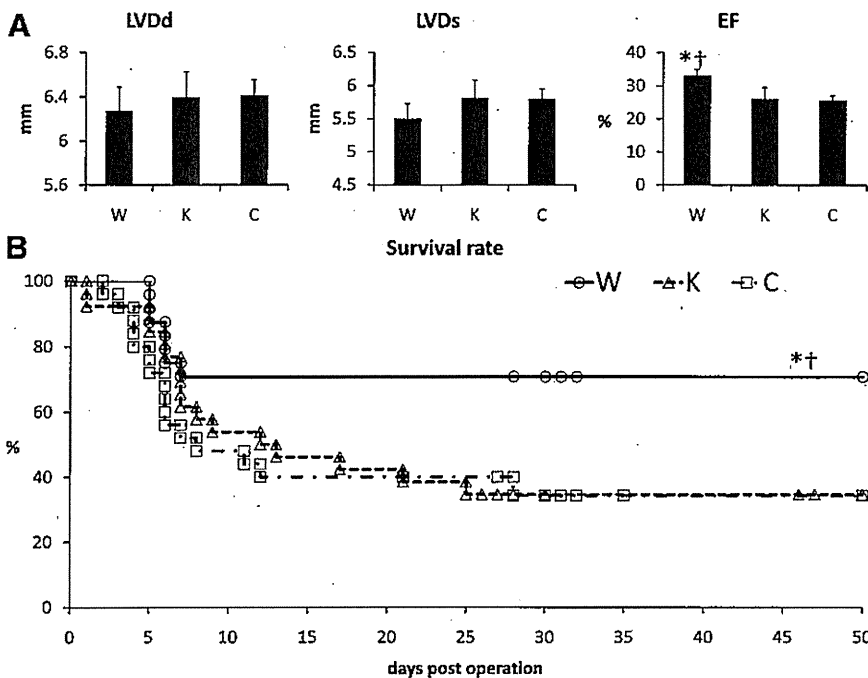


**Figure 6.** Wild-type induced adipocyte cell-sheet (WT-iACS) improved cardiac function and survival after myocardial infarction. **A**, Evaluation of cardiac performance 4 weeks after treatment (n=18 each). In the W group, the left ventricular end-systolic dimension was smaller and the ejection fraction significantly higher than in the other groups ( $P < 0.05$ , Kruskal-Wallis test). \* $P < 0.05$  versus C group. † $P < 0.05$  versus K group, post hoc Wilcoxon-Mann-Whitney *U* test. **B**, Survival rates after treatment. There was no significant difference between the C (n=25) and K groups (n=26). The W group (n=24) showed significantly better survival than the other groups ( $P < 0.05$ , overall log-rank test). \* $P < 0.05$  versus C group, † $P < 0.05$  versus K group, post hoc log-rank test.

inflammation, and amount of apoptosis. The beneficial effects of APN on inflammation after the iACS treatment may have led to the attenuated infarct size and suppressed the exacerbation of cardiac performance. In addition, APN has been shown to directly inhibit the hypertrophic response in myocytes.<sup>24</sup> Therefore, the combined direct and indirect actions of APN probably inhibit the development of pathological hypertrophy and preserve myocardial mass. Although we traced the iACS-derived APN by using APN-KO mice to demonstrate the APN delivery, HGF, VEGF, and other beneficial growth factors are probably also released constitutively by the iACS. Thus, iACS can provide a combined and balanced release of multiple paracrine mediators that may synergistically augment therapeutic benefits.<sup>20,23</sup>

On the other hand, APN is reported to have proangiogenic potential.<sup>9</sup> In fact, VEGF secretion from WT-iACS and KO-iACS were also greater compared with undifferentiated WT-SVF cell-sheet in this study. However, the capillary density in the treated myocardium, which was assessed by CD31 immunohistochemical labeling, was not higher at 28 days after WT-iACS transplantation, compared with post-KO-iACS transplantation and sham transplantation. These inconsistent findings may result from the AMI model in which neovascularization substantially occurs in the treated area, not allowing dissection of the slight difference in capillary density between the experimental groups. Rather, the findings of this study suggested that anti-inflammatory effects were the major mechanism for the improvement after WT-iACS transplantation in this model. Another disease model such as dilated cardiomyopathy and old myocardial infarction may be more appropriate to evaluate angiogenic property of iACS treatment.

The treatment strategy for AMI studied here is not directly applicable to the clinical arena, because the time required to isolate, cultivate, or manipulate cells *in vitro* is not available for AMI, which requires immediate treatment. However, the

finding that this therapy yielded marked cardioprotective effects through constitutive APN production should be beneficial for treating other types of cardiac pathologies, such as the chronic phase of MI, dilated cardiomyopathy, or myocarditis. In addition, this sophisticated cell-sheet, which elevates the systemic APN level for some time, might also be effective for treating systemic disorders such as obesity-linked cardiovascular or metabolic disorders, although this possibility will require further investigation.<sup>9,21</sup>

A potential limitation of this study is that the small sample sizes in our experiments limit their statistical power. Thus, the apparent absence of a statistical difference may be due to the lack of statistical power to detect small differences; therefore our negative results may have no meaning. Nevertheless, despite the small sample sizes, we at least clearly showed that APN was delivered by WT-iACS and that the therapeutic effect of WT-iACS implantation was attained through APN. Furthermore, we conducted multiple statistical tests for significance separately for each outcome in a univariate manner, although we adjusted for multiple pairwise testing between groups within each outcome. Such tests for multiple outcomes could lead to the inflation of the type I error probability in making treatment effect claims.

In the present study, we focused on the delivery of cytokines by iACS. However, we speculate that other mechanisms may also contribute to the functional recovery after iACS implantation. Tateno et al<sup>25</sup> clearly showed that cell transplantation induces the recipient tissue to produce angiogenic factors, including IL-1 $\beta$ , even though the transplanted cells do not produce sufficient levels of cytokines to promote angiogenesis directly. Similarly, iACS may stimulate recipient tissue, thus activating cells in the recipient to produce angiogenic cytokines. Further study will be required to elucidate what cross-talk occurs between the iACS and the recipient myocardium.

In summary, iACS may be a powerful DDS for cytokines, including APN, HGF, and VEGF. The implantation of iACS onto the infarcted mouse heart reduces the infarct size, inflammation, and LV remodeling. This method is probably adaptable as a novel DDS for treating heart failure.

### Acknowledgments

We thank Masako Yokoyama and Yoko Motomura for excellent technical assistance.

### Sources of Funding

This study was funded in part by a grant-in-aid for Scientific Research (22659251) from the Ministry of Education, Culture, Sports, Science, and Technology of Japan.

### Disclosures

Dr Shimizu is a consultant for CellSeed, Inc. Dr Okano is an Advisory Board Member in CellSeed, Inc, and an inventor/developer designated on the patent for temperature-responsive culture surfaces.

### References

- Hwang H, Kloner RA. Improving regenerating potential of the heart after myocardial infarction: factor-based approach. *Life Sci*. 2010;86:461–472.
- Vandervelde S, van Luyn MJ, Tio RA, Harmsen MC. Signaling factors in stem cell-mediated repair of infarcted myocardium. *J Mol Cell Cardiol*. 2005;39:363–376.
- Gnecchi M, Zhang Z, Ni A, Dzau VJ. Paracrine mechanisms in adult stem cell signaling and therapy. *Circ Res*. 2008;103:1204–1219.
- Herrmann JL, Abarbanell AM, Weil BR, Wang Y, Wang M, Tan J, Meldrum DR. Cell-based therapy for ischemic heart disease: a clinical update. *Ann Thorac Surg*. 2009;88:1714–1722.
- Miyagawa S, Saito A, Sakaguchi T, Yoshikawa Y, Yamauchi T, Imanishi Y, Kawaguchi N, Teramoto N, Matsuura N, Iida H, Shimizu T, Okano T, Sawa Y. Impaired myocardium regeneration with skeletal cell sheets—a preclinical trial for tissue-engineered regeneration therapy. *Transplantation*. 2010;90:364–372.
- Shimizu T, Sekine H, Yamato M, Okano T. Cell sheet-based myocardial tissue engineering: new hope for damaged heart rescue. *Curr Pharm Design*. 2009;15:2807–2814.
- Nakagami H, Morishita R, Maeda K, Kikuchi Y, Ogihara T, Kaneda Y. Adipose tissue-derived stromal cells as a novel option for regenerative cell therapy. *J Atheroscler Thromb*. 2006;13:77–81.
- Maeda K, Okubo K, Shimomura I, Funahashi T, Matsuzawa Y, Matsubara K. cDNA cloning and expression of a novel adipose specific collagen-like factor, ap1 (adipose most abundant gene transcript 1). *Biochem Biophys Res Commun*. 1996;221:286–289.
- Shibata R, Ouchi N, Murohara T. Adiponectin and cardiovascular disease. *Circ J*. 2009;73:608–614.
- Maeda N, Shimomura I, Kishida K, Nishizawa H, Matsuda M, Nagaretani H, Furuyama N, Kondo H, Takahashi M, Arita Y, Komuro R, Ouchi N, Kihara S, Tochino Y, Okutomi K, Horie M, Takeda S, Aoyama T, Funahashi T, Matsuzawa Y. Diet-induced insulin resistance in mice lacking adiponectin/acrp30. *Nat Med*. 2002;8:731–737.
- Planat-Benard V, Silvestre JS, Cousin B, Andre M, Nibbelink M, Tamarat R, Clergue M, Manneville C, Saillan-Barreau C, Duriez M, Tedgui A, Levy B, Penicaud L, Casteilla L. Plasticity of human adipose lineage cells toward endothelial cells: physiological and therapeutic perspectives. *Circulation*. 2004;109:656–663.
- Imanishi Y, Saito A, Komoda H, Kitagawa-Sakakida S, Miyagawa S, Kondo H, Ichikawa H, Sawa Y. Allogenic mesenchymal stem cell transplantation has a therapeutic effect in acute myocardial infarction in rats. *J Mol Cell Cardiol*. 2008;44:662–671.
- R Development Core Team. R: A language and environment for statistical computing. 2008. R Foundation for Statistical Computing; Vienna, Austria. ISBN 3-900051-07-0. <http://www.R-project.org>. Accessed August 3, 2011.
- Kondo K, Shibata R, Unno K, Shimano M, Ishii M, Kito T, Shintani S, Walsh K, Ouchi N, Murohara T. Impact of a single intracoronary administration of adiponectin on myocardial ischemia/reperfusion injury in a pig model. *Circ Cardiovasc Interv*. 2010;3:166–173.
- Davis ME, Hsieh PC, Grodzinsky AJ, Lee RT. Custom design of the cardiac microenvironment with biomaterials. *Circ Res*. 2005;97:8–15.
- Yla-Herttuala S, Martin JF. Cardiovascular gene therapy. *Lancet*. 2000;355:213–222.
- Joung YK, Bae JW, Park KD. Controlled release of heparin-binding growth factors using heparin-containing particulate systems for tissue regeneration. *Expert Opin Drug Deliv*. 2008;5:1173–1184.
- Allison SD. Analysis of initial burst in PLGA microparticles. *Expert Opin Drug Deliv*. 2008;5:615–628.
- Xia Z, Triffitt JT. A review on macrophage responses to biomaterials. *Biomed Mater*. 2006;1:R1–R9.
- Golocheikine A, Tiriveedhi V, Angaswamy N, Benschoff N, Sabarinathan R, Mohanakumar T. Cooperative signaling for angiogenesis and neovascularization by VEGF and HGF following islet transplantation. *Transplantation*. 2010;90:725–731.
- Hopkins TA, Ouchi N, Shibata R, Walsh K. Adiponectin actions in the cardiovascular system. *Cardiovasc Res*. 2007;74:11–18.
- Ouchi N, Walsh K. Adiponectin as an anti-inflammatory factor. *Clin Chim Acta*. 2007;380:24–30.
- Shibata R, Sato K, Pimentel DR, Takemura Y, Kihara S, Ohashi K, Funahashi T, Ouchi N, Walsh K. Adiponectin protects against myocardial ischemia-reperfusion injury through AMPK- and COX-2-dependent mechanisms. *Nat Med*. 2005;11:1096–1103.
- Shibata R, Ouchi N, Ito M, Kihara S, Shiojima I, Pimentel DR, Kumada M, Sato K, Schiekofer S, Ohashi K, Funahashi T, Colucci WS, Walsh K. Adiponectin-mediated modulation of hypertrophic signals in the heart. *Nat Med*. 2004;10:1384–1389.
- Tateno K, Minamino T, Toko H, Akazawa H, Shimizu N, Takeda S, Kunieda T, Miyauchi H, Oyama T, Takeda S, Kunieda T, Miyauchi H, Oyama T, Matsuura K, Nishi J-i, Kobayashi Y, Nagai T, Kuwabara Y, Iwakura Y, Nomura F, Saito Y, Komuro I. Critical roles of muscle-secreted angiogenic factors in therapeutic neovascularization. *Circ Res*. 2006;98:1194.

## SUPPLEMENTAL MATERIALS

**MS ID#: CIRCULATIONAHA/2010/009993/R1**

**MS TITLE: Induced Adipocyte Cell-Sheet Ameliorates Cardiac Dysfunction in Mouse Myocardial-Infarction Model - A Novel Drug Delivery System for Heart Failure**

### Materials and Methods

#### Preparation of Adipocyte cell-sheet

Stromal-vascular fraction (SVF) cells were enzymatically isolated from adipose tissues.<sup>1</sup> Briefly, inguinal adipose tissue was excised from wild type mice (WT; male C57BL/6J), APN knockout (KO) mice which were generated and backcrossed to C57BL/6J over 6 generations as described previously<sup>2</sup>, or from rats (3-week-old, male LEW/Sea). Adipose tissue was digested in Hank's balanced buffered saline (Sigma-Aldrich, MO, USA) containing 0.1% collagenase type II (Life Technologies, CA, USA) at 37°C with shaking vigorously for 1 hour. The adipose cell extracts were passed 100 µm and 70 µm filters, resuspended in Dulbecco's Modified Eagle's Medium (Life Technologies) containing 10% fetal bovine serum (Equitech-bio, TX, USA), 200 µM ascorbic acid (Sigma-Aldrich), and antibiotics (Life Technologies), then cultured on culture dishes (AGC Techno Glass, Chiba, Japan) at 37°C and 5% CO<sub>2</sub>. Twenty-four hours after plating, all the non-adherent cells were removed by washing. The SVF cells were cultured for 3 days in

the same medium. The SVF cells were then seeded at 7000 cells/cm<sup>2</sup> in an Upcell dish, which is coated with temperature-responsive polymers (CellSeed, Tokyo, Japan). The culture area was 1.9 cm<sup>2</sup> for mouse cells and 8.8 cm<sup>2</sup> for rat cells. Seven days after passage, the SVF cells were induced to differentiate into the adipogenic lineage by adding 0.87 μM insulin, 0.25 μM dexamethasone, 500 μM isobutylmethylxanthine (IBMX), and 5 μM Pioglitazone (Sigma-Aldrich) for 48 hours. Seven days after induction, the adipocytes were induced to spontaneously detach by placing the plates at 20 °C for 1 hour, yielding a scaffold-free sheet-shaped monolayer of induced adipocyte cell-sheet (iACS) that could be used as a graft. Finally, two iACS were layered to make a thicker sheet for grafting. Both WT mouse-derived iACS and APN-KO mouse-derived iACS were either assessed *in vitro* or labeled using a PKH26 red fluorescent linker kit (Sigma-Aldrich) prior to transplantation.

#### Enzyme-Linked Immunosorbent Assay

To determine the content of the secreted factors, enzyme-linked immunosorbent assays (ELISA) were performed. The collected culture supernatant of the WT-iACS, WT SVC cell-sheet or KO-iACS was centrifuged to remove debris and contaminating cells. For APN, samples were diluted 1:200 and analyzed (W, n=5; K, n=8). APN content of plasma samples from iACS-received APN-KO mice were analyzed with no dilutions (W 1 mo, n=4; W 3 mo, n=3; K

1 mo, n=4). An APN ELISA kit was purchased from Otsuka Pharmaceutical (Tokushima, Japan) according to the manufacturer's instructions. Content of HGF, VEGF, leptin, IL-6, IL-10, and TNF $\alpha$  in the culture supernatants were also analyzed by ELISA kit (R&D systems, MN, USA) with no dilutions (W, n=8-12; K, n=6-9).

### **Animal experiments**

Myocardial infarction (MI) model of mice was created by left anterior descending artery (LAD) ligation as described previously.<sup>3</sup> Mice (10-15-weeks old, male C57BL/6J) were anesthetized by inhalation of isoflurane (1.5%, 1L/min, Mylan Inc., Pittsburgh, PA) provided by an anesthetic gas machine (DS Pharma, Osaka, Japan). The anesthetized mice were intubated in an endotracheal manner, and positive pressure ventilation was maintained with a ventilator (room air, 90 cycles/minutes, tidal volume 1 ml, Shinano, Tokyo, Japan). Then, the heart was exposed through a left lateral thoracotomy. With minimal manipulation of the fat pad surrounding the heart, the LAD component could easily be visualized. LAD was ligated with an 8-0 prolene suture (Johnson & Johnson, NJ, USA) at 1 mm distal to the left atrial appendage, immediately after bifurcation of the major left coronary artery. The myocardial ischemic area was visually assessed, to confirm that the LAD ligation had consistent ischemic effects. Procedure-related mortality, which occurred prior to chest closure, was consistently 6% in all the experimental

groups, suggesting a consistent level of acute myocardial ischemia. Within 5 minutes after LAD ligation, the mice were randomly allocated into 3 groups; those that underwent transplantation of WT-iACS (W group; n=40); those that underwent transplantation of KO-iACS (K group; n=40) and those that underwent sham transplantation (C group; n=43). The pericardium was closed to prevent the dislocation of iACS. The mice were allowed to recover under care. In the experiment of iACS implantation to APN-KO mice, MI was not induced.

The mice were euthanized at 2 and 28 days after surgery by intravenous injection of pentobarbital (200 mg/kg body weight; DS Pharma) and 30 mM of potassium chloride (Wako Pure Chemical Industries, Osaka, Japan) to cause cardiac arrest in diastole under terminal anesthesia, and the heart was excised.

On day 2, the specimens for RNA analyses were cut transversely, and then the apex-side specimens were dissected to remove the right ventricular free wall, and part in the three pieces of infarction, peri-infarction, and remote, and soaked in RNA Later (Qiagen, Hilden, Germany, W, n=4; K, n=4; C, n=6). The specimens for CD11b staining were cut into 4 segments, embedded in OCT compound (Sakura Finetek Japan, Tokyo, Japan), and snap frozen in liquid nitrogen (W, n=4; K, n=4; C, n=6). The appropriate segments used for gene expression or histological analyses on day 2 were also used for TTC staining (W, n=8; K, n=7; C, n=9). The specimens used for the cytokine-array analysis were snap frozen in liquid nitrogen on day 2 (W,

n=4; K, n=5; C, n=6). The remaining mice were used for survival-rate analysis (W, n=24; K, n=26; C, n=25), but cases of accidental death were excluded. Twenty-eight days after treatment, 18 mice from each group were randomly chosen for cardiac performance analysis by echocardiography. Histological analyses were also performed at 28 days (W, n=6; K, n=8; C, n=5).

MI was also created in rats (8-week-old, female LEW/Sea) by the same method described above, except the tidal volume was 4 ml. Five minutes after LAD ligation, either two layers of iACS were transplanted onto the LV (n=9) or a sham transplantation was performed (n=6). Four weeks after the operation, a hemodynamic assessment was performed.

### **Quantitative real time PCR**

Total RNA was isolated from the stored specimens using the RNeasy Mini Kit (Qiagen) and reverse transcribed with Ominiscript Reverse transcriptase (Qiagen). Quantitative PCR was performed with the ABI 7500 Fast Real-Time PCR System (Life Technologies) using Taqman Universal Master Mix (Life Technologies). Measurement copy number of mRNA was performed in triplicate. The primers and probes are shown in the Table. All probes were designed with a 5' fluorogenic probe 6FAM and a 3' quencher TAMURA. The results were normalized to glyceraldehyde-3-phosphate dehydrogenase (GAPDH).



### Determination of infarct size

Freshly excised hearts from the W, K, and C groups 2 days after transplantation were washed in PBS and dissected into four transverse slices. The slices were then stained for 5 min at 37°C with 1% 2,3,5-triphenyltetrazolium chloride (TTC; Sigma-Aldrich) to determine the infarct area. The stained slices were photographed, and then the infarct area was determined by computerized planimetry using MetaMorph Software (Molecular Device, CA, USA).

### Histological analysis

Histological analyses of the hearts were performed 2 and 28 days after transplantation. The hearts and cell-sheets were cut into 8- $\mu$ m sections. The sections were stained with antibodies for APN (1:1000 dilution; Otsuka Pharama), CD11b (1:100 dilution; Abcam, Cambridge, UK), or CD31 (1:200 dilution; Abcam). The secondary antibody was Alexa 488 goat anti-rabbit (1  $\mu$ g/ml; Life Technologies). Counterstaining was with 6-diamidino-2-phenylindole (DAPI; 1  $\mu$ g/ml; Life Technologies). Images were captured by fluorescence microscopy (Keyence, Osaka, Japan). Routine hematoxylin-eosin staining was performed. Masson's trichrome staining was performed to analyze the collagen accumulation. The collagen volume fraction in the peri-infarct area was calculated as the percentage of the myocardium. The data were collected

from 10 individual views per heart at a magnification of  $\times 200$ . Furthermore, the heart sections were stained with Periodic acid-Schiff (PAS) to assess the cardiomyocyte size. Cardiomyocyte size at a magnification of  $\times 400$  was average from 50 myocytes per sample. MetaMorph Software was used for quantitative morphometric analysis.

### **Myocardial echocardiography**

Echocardiography examinations were performed 4 weeks after cell transplantation by an investigator blinded to the group identities (n=18 each). Two-dimensional, targeted M-mode tracings were obtained at the level of the papillary muscles with an echocardiography system equipped with a 12-MHz transducer (GE Healthcare, WI, USA). The left ventricular (LV) dimensions were measured following the method of the American Society of Echocardiology from at least 3 consecutive cardiac cycles. Three readings were obtained from each mouse and averaged. The LV ejection fraction (EF) was calculated as  $(LVDd^3 - LVDs^3) / LVDd^3 \times 100$ , where LVDd is the LV end-diastolic dimension and LVDs is the LV end-systolic dimension.<sup>4</sup>

### **Hemodynamic analysis**

Four weeks after LAD ligation and cell-sheet transplantation, rats (iACS-treated group, n=9; sham-treated group, n=6) were anesthetized and ventilated. A silk thread was placed under the

inferior vena cava to change the LV preload. The conductance catheter (Unique Medical, Tokyo, Japan) was inserted through the LV apex toward the aortic valve along the longitudinal axis of the LV cavity, then fixed. A Millar 1.4 F pressure-tip catheter (Millar Instruments, TX, USA) was also inserted from the LV anterior and fixed. The conductance system and the pressure transducer controller (Integral 3; Unique Medical) were set as previously reported.<sup>5</sup> The conductance, pressure, and intracardiac electrocardiographic signals were analyzed with the Integral 3 software. The baseline indices were initially measured under stable hemodynamic conditions, then the pressure-volume loop was drawn during inferior vena caval occlusion, and analyzed. The following indices were calculated:  $dp/dt_{max}$ ,  $dp/dt_{min}$ , the time constant of isovolumic relaxation ( $\tau$ ), and the end-systolic pressure-volume relationship (ESPVR).

#### **Evaluation of survival rate after the operation**

To evaluate the life-saving effect of the implantation, survival rates were determined. The mice were housed for 50 weeks after the operation. The survival rates of the mice in the W, K, and C groups were evaluated by the Kaplan–Meier method. The comparison among the three groups was analyzed by the overall log-rank test, and the pairwise comparisons were performed by log-rank test with the Benjamin-Hochberg multiplicity correction.

### **Cytokine antibody array**

Protein was isolated from the stored specimens of mouse heart at  $-80^{\circ}\text{C}$ . The whole heart tissues were homogenized in Tissue Extraction Reaction Reagent I (Life Technologies), centrifuged, and finally passed 0.22- $\mu\text{m}$  filter (Millipore, MA, USA). Protein contents were measured by Milliplex Mouse Cytokine/Chemokine Panel Pre-mixed 32Plex, according the manufacturer's instructions (Millipore).